

1 **Electrocoagulation: simply a phase separation technology?**
2 **The case of bronopol compared to its treatment by EAOPs**

3
4 **Elvira Bocos^a, Enric Brillas^b, M. Ángeles Sanromán^a, Ignasi Sirés^{*,b}**

5
6 ^a Department of Chemical Engineering, University of Vigo, Isaac Newton Building, Campus
7 As Lagoas Marcosende 36310, Vigo, Spain

8 ^b Laboratori d'Electroquímica dels Materials i del Medi Ambient, Departament de Química
9 Física, Facultat de Química, Universitat de Barcelona, Martí i Franquès 1-11, 08028
10 Barcelona, Spain

11
12
13
14
15 **Paper submitted to be published in *Environmental Science & Technology***

16
17
18
19
20
21 *Corresponding author:

22 *E-mail address:* i.sires@ub.edu (Ignasi Sirés)

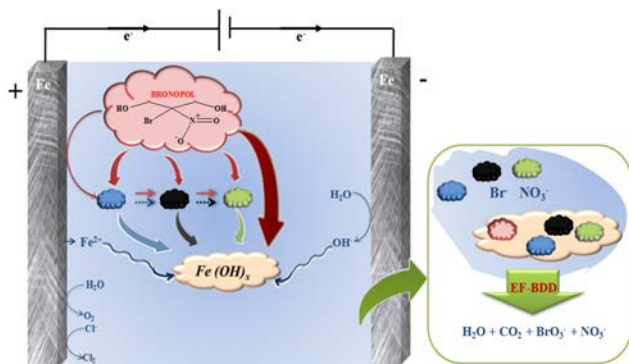
23 Tel.: +34 934039240; fax: +34 934021231.

25 **ABSTRACT**

26 Electrocoagulation (EC) has long been considered a phase separation process, well suited for
27 industrial wastewater treatment since it causes a quick, drastic decay of organic matter
28 content. This research demonstrates that EC also behaves, at least for some molecules like the
29 industrial preservative bronopol, as an effective transformation technology able to yield
30 several breakdown products. This finding has relevant environmental implications, pointing to
31 EC as a greener process than described in literature. A thorough optimization of EC was
32 performed with solutions of bronopol in a simulated water matrix, yielding the complete
33 disappearance of the parent molecule within 20 min at 200 mA ($\sim 20 \text{ mA/cm}^2$), using Fe as the
34 anode and cathode. A 25% of total organic carbon (TOC) abatement was attained as
35 maximum, with bronopol being converted into bromonitromethane, bromochloromethane,
36 formaldehyde and formic acid. N atoms were accumulated as NO_3^- , whereas Br^- was stable
37 once released. This suggests that mediated oxidation by active chlorine, as well as by
38 hydroxyl radicals resulting from its reaction with iron ions, is the main transformation
39 mechanism. Aiming to enhance the mineralization, a sequential combination of EC with
40 electro-Fenton (EF) as post-treatment process was proposed. EF with boron-doped diamond
41 (BDD) anode ensured the gradual TOC removal under the action of $\bullet\text{OH}$ and $\text{BDD}(\bullet\text{OH})$, also
42 transforming Br^- into BrO_3^- .

43

44 **TABLE OF CONTENTS (TOC) ART**



45

46

47 INTRODUCTION

48 Since its first application for sewage treatment in 1889,¹ electrocoagulation (EC) has
49 been considered by the scientific and industrial communities as a mere separation technology
50 that does not alter the structure of the parent organic molecules, simply causing their removal
51 by agglomeration with metal hydroxide flocs to form a contaminated sludge.^{2,3} Recently,
52 there has been renewed scientific and technological interest in this process owing to the
53 increasing demand of simple but highly effective water treatment technologies, as well as its
54 suitability to be powered by renewable electricity sources⁴ and be conceived as small-scale
55 decentralized units.⁵ Companies like Powell Water, WaterTectonics or Elgressy offer
56 solutions based on EC for mining and oil and gas markets, among others, whereas several
57 projects including REWAGEN, EColoRo and ECOWAMA have been funded as part of
58 Europe's FP7 and Horizon 2020 research programs. EC has therefore been brought to the
59 forefront and a more thorough investigation of its particularities is needed.

60 It has been shown that during EC in Cl⁻-containing media, this anion can be oxidized at
61 the anode surface to form active chlorine (Cl₂, HClO/ClO⁻), which is widely used as
62 oxidation and disinfection agent. For example, it has been mentioned that it contributes to dye
63 decolorization.⁶ This assumption has been rarely verified by measuring the transformation
64 products, although in a recent study some of us showed the accumulation of chlorobenzene
65 derivatives during the EC of the dye Tartrazine.⁷ To date, this phenomenon constitutes the
66 only evidence that EC behaves as a partial transformation technology.

67 Usually, total organic carbon (TOC) removal is not feasible by EC, thus being required
68 a post-treatment. EC has been combined with ozonation⁸ and photocatalysis,⁹ but a better
69 suited combination arises from coupling with Fenton-based processes to take advantage of the
70 metal ions dissolved during the EC step.¹⁰ On the other hand, great progress has been made in
71 developing the so-called electrochemical advanced oxidation processes (EAOPs). The effect

72 of the main operation parameters on their performance has been thoroughly evaluated.¹¹⁻¹³
73 Among them, electro-Fenton (EF) process has shown large ability to oxidize organic matter
74 within a shorter time. In EF, H₂O₂ is electrogenerated on site in acidic solutions from the two-
75 electron O₂ reduction at a suitable cathode material. In the presence of Fe²⁺, the occurrence of
76 Fenton's reaction yields •OH in the bulk.¹⁴ In undivided electrolytic cells, M(•OH) is also
77 generated on the anode surface (M),¹⁵ which can be a boron-doped diamond (BDD),¹⁶⁻²²
78 Pt,^{16,17,20} graphite^{19,23} or dimensionally-stable anode (DSA).^{17,18,24,25} As demonstrated from
79 studies on integrated water networks,²⁶ EC is an optimum candidate for coupling strategies. It
80 has been employed as a pre-treatment before use of electro-oxidation (EO).²⁷⁻²⁹ Recently, we
81 reported for the first time the sequential combination of EC and EAOPs based on Fenton's
82 reaction. EC induces the large coagulation of organic matter as well as the accumulation of
83 metal ions, which can be further used to oxidize the remaining organic matter by EF as post-
84 treatment.^{7,30}

85 Bronopol is widely used as antiseptic and preservative in products like cosmetics and
86 toiletries since it prevents bacterial growth. It is readily soluble in water, which justifies its
87 use in aquaculture.³¹ However, under certain conditions it decomposes, thus being considered
88 a formaldehyde releaser³² that can eventually yield nitrosamines. All these products are
89 known human carcinogens and, moreover, bronopol is considered a skin chemical sensitizer
90 that causes allergic contact dermatitis.³² Formaldehyde is subject to regulation due to its toxic
91 properties, which has triggered the use of formaldehyde-releasing agents as surrogates that are
92 also under restriction in Europe.³³ Preservatives have been found in concentrations up to mg/L
93 and µg/L in industrial effluents as well as in influents of wastewater treatment facilities,³⁴
94 although no much information is available on their occurrence and toxicity. Bronopol may be
95 hydrolyzed in water to yield several products, but it is only slowly degraded at certain pH
96 values and usually requires a few days or weeks.^{35,36} Temperature and sunlight/UV radiation

97 may affect the decay rate of bronopol as well.³⁶ To our knowledge, no investigation has
98 addressed the use of advanced oxidation processes and electrochemical technologies for
99 treating bronopol in water, whereas only some irrelevant study reported its redox activity in
100 environmental samples. Ergo, it is an optimum candidate to gain further understanding on EC.

101 The present contribution gives detailed insight into the potentialities of EC as a
102 transformation technology, which could confer a greater environmental compatibility because
103 of a cleaner sludge. Solutions of bronopol in a simulated water matrix have been
104 electrocoagulated under different conditions to optimize the process. The decay of the
105 pollutant as well as its mineralization and fate of heteroatoms has been studied by high-
106 performance liquid chromatography (HPLC), TOC analysis and ion chromatography (IC),
107 whereas transformation products have been identified by gas chromatography-mass
108 spectrometry (GC-MS). Likewise, bronopol has been degraded by EF using an air-diffusion
109 cathode and different anodes, which was followed by coupling between EC and EF to achieve
110 a greater conversion of the pollutant and products. Comparative electrolyses were performed
111 in Na₂SO₄ as an inert electrolyte and a reaction route for the sequential treatment is proposed.

112 **EXPERIMENTAL SECTION**

113 **Chemicals.** Bronopol (2-bromo-2-nitro-1,3-propanediol, 98%), bromonitromethane
114 (90%) and 2-bromoethanol (95%) of reagent grade were purchased from Sigma-Aldrich and
115 used as received. Formaldehyde, formic acid, perchloric and sulfuric acids (used to adjust the
116 pH prior to EF treatment), anhydrous sodium sulfate (background electrolyte), Fe(II) sulfate
117 heptahydrate (catalyst source for single EF) as well as ammonium oxalate, potassium bromate
118 and sodium nitrate, nitrite, chloride and bromide employed in IC and salts needed for the
119 simulated water matrix were analytical grade from Fluka, Acros Organics and Sigma-Aldrich.
120 All solutions used for calibration of instruments were prepared with ultrapure water from a

121 Millipore Milli-Q system (resistivity >18 MΩ cm at room temperature). A simulated water
122 matrix mimicking the ionic content of real water from a wastewater treatment facility located
123 near Barcelona (Spain) was used for the electrolyses of bronopol. For this, pure salts
124 accounting for 1.3 mM SO₄²⁻, 11.5 mM Cl⁻, 0.02 mM NO₃⁻, 1.5 mM NH₄⁺, 11.6 mM Na⁺
125 and 1.0 mM K⁺ ions were added to ultrapure water, yielding a solution of 1.7 mS/cm at pH
126 6.5 (hereby called natural pH). For comparison, some electrolyses were performed in 10 mM
127 Na₂SO₄ (same conductivity).

128 **Electrolytic systems.** The experiments were done in an open, undivided glass cell of
129 150 mL capacity with a double jacket for circulation of water thermostated at 35 °C, under
130 vigorous stirring provided by a magnetic PTFE follower. For the EC trials, the anode was a
131 pure Fe, pure Al or stainless steel (AISI 304 and 316L) plate with immersed dimensions of
132 3.0 cm × 1.5 cm, 0.25 cm thickness (all sides exposed to solution). The same materials with
133 analogous dimensions were tested as cathode. One or more electrode pairs were placed
134 alternately in parallel with an interelectrode gap from 1.0 to 4.0 cm, employing a monopolar
135 parallel electrical configuration. This connection mode was preferred because, at laboratory
136 scale, it avoids issues with bypass current. At industrial scale, it allows controlling the anode
137 consumption and its periodic replacement, although bipolar connection is also widespread
138 since it requires the use of fewer connections and a high voltage / low current power supply.
139 Before first use, all electrodes were properly cleaned and then activated with a 0.1 M NaOH
140 or H₂SO₄ solution. For the EF process, the anode (3 cm²) was either a Pt sheet of 99.99%
141 purity supplied by SEMPSA (Barcelona, Spain), a BDD thin-film electrode supplied by
142 NeoCoat (La-Chaux-de-Fonds, Switzerland) or a DSA-O₂ (IrO₂-based anode) or DSA-Cl₂
143 (RuO₂-based anode) plate from NMT Electrodes. The cathode was a 3 cm² carbon-PTFE air-
144 diffusion electrode supplied by E-TEK (Somerset, NJ, USA), mounted as described elsewhere
145 and fed with air pumped at 1 L/min for continuous H₂O₂ generation.¹⁴ The interelectrode gap

146 was about 1.0 cm. Before first use, a preliminary polarization was done in 0.05 M Na₂SO₄ at
147 100 mA cm⁻² for 180 min to remove the impurities of the BDD surface and the activation of
148 the air-diffusion electrode.

149 **Analytical procedures.** The electrical conductance and pH were measured with a
150 Metrohm 644 conductometer and a Crison 2000 pH-meter, respectively. Constant current
151 electrolyses were performed with an Amel 2049 potentiostat-galvanostat and the potential
152 difference between the anode and cathode (E_{cell}) was provided by a Demestres 601BR digital
153 multimeter. The mineralization of solutions was assessed from their TOC abatement,
154 determined on a Shimadzu TOC-VCNS analyzer (Text S1 of the Supporting Information, SI).

155 The time course of the concentration of bronopol was followed by reversed-phase
156 HPLC upon injection of 10 μ L aliquots into a Waters 600 LC fitted with a Waters Spherisorb
157 ODS2-C18 5 μ m, 150 mm \times 4.6 mm, column at 25 $^{\circ}$ C and coupled to a Waters 996
158 photodiode array detector set at 210 nm. All the samples withdrawn from treated solutions
159 were filtered with Whatman 0.45 μ m PTFE filters. The analyses were carried out isocratically
160 using a 5:95 (v/v) acetonitrile/water (0.1% H₃PO₄) mixture as mobile phase at 1.0 mL/min.
161 The corresponding retention time (t_{R}) for bronopol was 9.8 min. Generated aliphatic
162 carboxylic acids were identified and quantified by ion-exclusion HPLC using the same
163 chromatograph, fitted with a Bio-Rad Aminex HPX 87H, 300 mm \times 7.8 mm, column at 35 $^{\circ}$ C
164 and the detector set at $\lambda = 210$ nm. A 4 mM H₂SO₄ solution eluted at 0.6 mL/min was used as
165 mobile phase. In these chromatograms, a well-defined peak appeared at $t_{\text{R}} = 13.6$ min for
166 formic acid. Inorganic anions accumulated in the electrolyzed solutions were determined by
167 IC upon injection into a Shimadzu 10Avp LC, using an anion-exchange column (Text S2 in
168 SI).

169 For a more complete identification of reaction products, GC-MS analysis was performed
170 with an Agilent Technologies system composed of a 6890N gas chromatograph coupled to a

171 5975C mass spectrometer operating in EI mode at 70 eV. A non-polar Teknokroma Sapiens-
172 X5ms and a polar HP INNOWax column, both of 0.25 μm , 30 m \times 0.25 mm, were used (Text
173 S3 in SI).

174 H_2O_2 concentration was determined from the light absorption of its Ti(IV) colored
175 complex at $\lambda = 408$ nm, measured on a Shimadzu 1800 UV/Vis spectrophotometer at 25 $^\circ\text{C}$.³⁷
176 Active chlorine produced was determined by the *N,N*-diethyl-*p*-phenylenediamine (DPD)
177 colorimetric method (Text S4 in SI).³⁸ Quantitative analysis of soluble iron accumulated in
178 electrocoagulated solutions was performed by inductively-coupled plasma (ICP-OES) using
179 the Optima 3200L spectrometer.

180 The electrochemical characterization was carried out by linear sweep voltammetry
181 (LSV) with an Autolab PGSTAT30 instrument (Text S5 in SI).

182 Solutions of 100-150 mL with 100 mg/L TOC (2.78 mM of bronopol) in 10 mM
183 Na_2SO_4 or in the simulated water matrix were treated by single EC (at natural pH) and
184 EAOPs (at pH 3.0). In EC, the effect of electrode material and pair number, interelectrode gap
185 and applied current was thoroughly studied. In the EAOPs, pH was fixed at 3.0 because this
186 was found as optimum for the EF treatment with air-diffusion cathode.¹⁴ To perform the
187 sequential EC/EF, EC-treated solutions were centrifuged for 5 min at high speed to easily
188 withdraw the supernatant to be further treated by EF upon pH adjustment to 3.0.

189 **RESULTS AND DISCUSSION**

190 **Separation and transformation ability of EC for bronopol solutions in simulated**
191 **water.** Once the stability of 2.78 mM bronopol solutions in simulated water and 10 mM
192 Na_2SO_4 at natural pH as well as at pH 3.0 was verified for 480 min by TOC and HPLC
193 measurements, we could establish that the changes occurring during the subsequent
194 electrochemical treatments arise from specific phenomena different from hydrolysis or

195 decomposition that have been reported in natural water after a few days or weeks. A first
196 series of EC experiments was then carried out aiming to find the most suitable anode and
197 cathode materials. In the literature, it has been described that it does not exist a rule to ensure
198 which material may provide larger decontamination for a given pollutant or wastewater.
199 However, focusing on the anode selection, Fe and Al tend to be considered as the materials of
200 choice. [SI Figure S1](#) shows the percentage of TOC removal reached at 60 min using different
201 anode/cathode combinations with 1.0 cm of interelectrode distance for the EC treatment of
202 bronopol in simulated water at natural pH and 200 mA. As can be seen in [SI Figure S1a](#), the
203 Fe/Fe pair yielded the greatest TOC removal among all electrode pairs under study (ca. 28%),
204 being much larger than that obtained from other combinations. The use of stainless steel
205 anodes could, in some cases, yield around 20% of TOC abatement, whereas the worse results
206 were achieved using an Al anode. Hence, it is clear that freshly formed amorphous iron
207 hydroxide flocs, which are fractal and highly porous,³ act as “sweep flocs” with large surface
208 areas, being beneficial for a quick adsorption of soluble organic compounds contained in
209 solution. Since bronopol is a charged molecule, electrostatic attraction may also contribute
210 decisively to its enhanced removal, as demonstrated from additional chemical coagulation
211 trials carried out independently using iron hydroxides. On the other hand, the larger tendency
212 of pure Fe to become electro-oxidized to Fe^{2+} , compared to stainless steel anodes, explains its
213 superior performance as the anode material, whereas the use of Fe cathode also favors the
214 larger release of iron ions from its chemical dissolution. The value of the potential difference
215 between the anode and cathode in each system, as well as the local passivation of the
216 electrode surface (no evidences were provided by the potential differences), are also important
217 parameters that may exert large influence on the release of metal ions and the consequent
218 variation of ionic strength and formation of particle aggregates.

219 Another relevant finding comes from the only partial TOC removal. If bronopol tends to
220 become electrocoagulated, as shown above, a much larger abatement would be expected since
221 coagulants are continuously produced in the presence of Fe^{2+} and OH^- generated at the
222 electrodes. The presence of nitrate ions, which are known to be detrimental for oxidizing an
223 iron electrode, in the simulated water cannot justify the formation of a passive layer because
224 their content is really low. The stabilization of TOC content from 60 min can thus be
225 accounted for by the accumulation of oxidation/reduction by-products that are not readily
226 coagulable and remain in solution, as will be further demonstrated below. In other words, it
227 seems that EC cannot be simply considered a separation technology, but also a transformation
228 one.

229 Note also that the fact that the Fe/Fe couple is the optimum one turns out to be
230 beneficial because: (i) it allows polarity reversal at industrial scale, which prevents electrode
231 scaling and fouling from organic layers, and (ii) iron ions accumulated in solution are the
232 preferred ones for coupling Fenton-based post-treatments, as explained later. Hereby, the
233 effect of experimental variables on EC using a Fe/Fe pair was studied with the same solution
234 composition. [Figure 1a](#) depicts the influence of applied current and interelectrode distance
235 using one single pair of electrodes, as well as the effect of the number of electrode pairs on
236 percentage of TOC removal attained at 60 min. In all these trials, conductivity increased from
237 1.7 to ca. 2.3 mS/cm, whereas pH varied from 6.5 to 8.0-8.5. As can be observed, increasing
238 percentage of TOC removal of ca. 14%, 17%, 28% and 30% were achieved at 50, 100, 200
239 and 300 mA, respectively, using one pair of electrodes at 1.0 cm. The expected trend is
240 reached within the range 50-200 mA (apparent current density of $\sim 5\text{-}20 \text{ mA/cm}^2$), since a
241 current increase leads to a greater production of Fe^{2+} and OH^- that ends in larger amounts of
242 coagulant $\text{Fe}(\text{OH})_x$. Furthermore, a greater applied current enhances the generation of Cl_2
243 from Cl^- contained in the simulated water (10 mM) via eq 1. This species, along with

244 HClO/CIO⁻ formed in the bulk upon Cl₂ dissolution, might potentially contribute to the
245 transformation of bronopol into molecules with a lower ability to coagulate, as for example
246 organochlorinated products.



248 A much less significant enhancement of decontamination was obtained by applying 300
249 mA. This can be explained by the excessive production of Fe²⁺ ions, which quickly form
250 massive hydroxide particles without ideal size and porosity and thus, with no time to entrap
251 an additional amount of organic matter. This hypothesis was ascertained from ICP
252 measurements, which yielded only 0.8 mg/L of dissolved iron at 300 mA, whereas up to 11,
253 22 and 62 mg/L were accumulated at 200, 100 and 50 mA, respectively. Therefore, the
254 optimal current value was 200 mA, ensuring the best dosage of coagulant species and
255 favoring the best growth of aggregates formed between hydroxydes and organic molecules.
256 Based on the anode weight loss upon the electrolysis at this current and according to
257 Faraday's law, current efficiency for anode dissolution was 100%, which suggests a
258 negligible contribution from O₂ evolution reaction.

259 The influence of the interelectrode distance was subsequently studied using the Fe/Fe
260 couple at 200 mA. [Figure 1a](#) shows no amelioration at 2.0 and 3.0 cm, whereas a slightly
261 higher TOC removal of 33% was reached at 4.0 cm. However, this occurred in concomitance
262 with a significant increase of potential difference due to the larger ohmic drop, which is
263 detrimental for future scale-up of this technology. A distance of 1.0 cm was considered to
264 yield the most well-balanced EC treatment, being chosen to test the effect of the number of
265 electrode pairs. Under the same conditions, the use of two Fe anodes and two Fe cathodes in
266 parallel-plate arrangement yielded a very similar TOC abatement of 25% at 60 min. This
267 confirms that, for the electrolytic cell employed in this study, such EC conditions are really
268 preferable since they promote the most efficient formation of coagulants and oxidants. This

269 latter configuration with four electrodes was then preferred to pursue the investigation, being
270 the most convenient at industrial scale because the anodes will exhibit longer service life due
271 to their slower dissolution. Consequently, the cost related to maintenance and replacement
272 will be significantly lower. Figure 1b shows the TOC vs time profile for the optimum EC
273 treatment with two Fe pairs. As can be seen, TOC content decreases gradually, with no
274 significant additional decontamination after 60 min. ICP measurements confirmed the
275 accumulation of up to 11 mg/L of dissolved iron in the final solution, as explained above.

276 The vast majority of studies dealing with EC just focus on the evolution of the global
277 organic matter content. Unfortunately, this gives an incomplete idea of the underlying
278 mechanisms occurring in this process. Here, the time course of bronopol concentration during
279 the optimum EC treatment of Figure 1b was evaluated by HPLC. Figure 2 reveals its total
280 disappearance after 20 min, which demonstrates the ability of EC technology to transform the
281 parent molecule into by-products that are accumulated in the solution bulk because they do
282 not coagulate. Although Cl_2 accumulation from eq 1 is thought to be rather slow because
283 current efficiency corresponding to anode dissolution is almost 100% under the adopted
284 conditions, it can be plausibly stated that the main oxidants are: (i) active chlorine, which may
285 promote the formation of chloroderivatives, and (ii) $\bullet\text{OH}$ formed in the bulk from Fenton-like
286 reaction between active chlorine (assuming the role of H_2O_2) and iron ions.^{39,40} The formation
287 of small amounts of weaker radical species like $\text{HO}_2\bullet$, $\text{H}\bullet$ and $\text{Cl}\bullet$ upon homogeneous and
288 heterogeneous reactions cannot be discarded either. In contrast, additional tests have revealed
289 that neither Fe^{2+} nor Fe^{3+} ions are able to oxidize the parent compound. The oxidants are then
290 able to convert bronopol into other molecules, but they are not powerful enough to further
291 mineralize them, as confirmed from the stable TOC values after 60 min. The analysis of
292 bronopol decay fits quite well to a pseudo-first-order kinetics, which would partly agree with

293 a constant generation of coagulant and oxidant species from electrode reactions that are
294 directly controlled by applied current.

295 The disappearance of bronopol at 20 min was corroborated by GC-MS analysis.
296 Bronopol (m/z 170, 152, 135), which was not detected after that time, yielded
297 bromonitromethane and bromochloromethane as brominated products that were also removed
298 within 20 min. Note that the formation of chloroderivatives confirms the partial contribution
299 of active chlorine (C_2 , $HClO/ClO^-$) to bronopol oxidation. Unlike many studies focused on
300 the environmental fate of bronopol, the formation of 2-bromoethanol was discarded because it
301 was not found by either HPLC or GC-MS. Although no brominated molecules were
302 accumulated at the end of the EC treatment (60 min), GC-MS confirmed the presence of other
303 organic by-products like formic acid and formaldehyde. The formation of the latter compound
304 from bronopol has been reported elsewhere,^{32,35,36,41} and it was verified from headspace
305 analysis upon injection without solvent delay at near-ambient temperature, in order to avoid
306 artifacts from GC-MS analysis.

307 The time course of Br^- ion during the same optimum EC trial depicted in the inset of
308 [Figure 2](#) agrees with the absence of organobrominated compounds after 20 min, as deduced
309 from the gradual accumulation of Br^- along the electrolysis to attain the maximum value of
310 2.78 mM Br^- at that time, whereupon it remained constant. In addition, the treatment of a
311 solution containing 2.78 mM NaBr instead of bronopol under analogous conditions informed
312 about the stability of Br^- ion in this EC system, which suggests the direct release of the anion
313 from oxidized organobrominated molecules, thus discarding BrO_3^- formation followed by
314 cathodic reduction.

315 **Effect of the anode material on the performance of electro-Fenton treatment of**
316 **bronopol solutions.** Once demonstrated that EC is not simply a separation process, it is
317 interesting to compare its oxidation power with that of two widespread EAOPs, namely EO

318 with H₂O₂ electrogeneration (EO-H₂O₂) and EF. First, the electrolysis of simulated water at
319 pH 3.0 was performed by EO-H₂O₂ and EF at 100 mA using an air-diffusion cathode and four
320 different anodes in order to compare their ability to accumulate H₂O₂. SI Figure S2 shows the
321 time course of H₂O₂ in EO-H₂O₂, which is < 7 mM at 480 min in all cases. This value is much
322 lower than reported for analogous trials in 0.05 M Na₂SO₄ (i.e., > 15 mM) due to its partial
323 destruction by active chlorine.⁴² The largest accumulation was achieved with BDD anode,
324 being much lower with Pt and IrO₂-based anodes. In experiments with the RuO₂-based anode,
325 H₂O₂ became totally consumed by active chlorine, which agrees with the greater active
326 chlorine concentration produced (1-3 mM). It is known that DSA-type anodes are well suited
327 for electrochemical hypochlorite production from very dilute chloride solutions.⁴³ In contrast,
328 BDD is usually preferred for treating organic pollutants, since it: (i) yields a higher H₂O₂
329 concentration that is beneficial for EF, and (ii) generates lower amounts of chlorinated
330 radicals that are less oxidizing than hydroxyl radicals formed from eq 2. This anode has then
331 been chosen to study the performance of EAOPs.



333 The ability of EO-H₂O₂ and EF with a BDD/air-diffusion cell to degrade 2.78 mM
334 bronopol was investigated in simulated water, as well as in 10 mM Na₂SO₄ to assess the
335 effect of ion content and determine the fate of released Br⁻. Figure 3a illustrates the
336 mineralization ability of both EAOPs in two water matrices at 100 mA. All treatments were
337 able to attain a TOC removal > 90% at 480 min, although two main conclusions can be drawn
338 from these curves: (i) EF with 0.50 mM Fe²⁺ performs better than EO-H₂O₂, which is
339 expected from the concomitant action of hydroxyl radicals formed at the anode surface from
340 eq 2 and in the bulk from Fenton's reaction (eq 3), and (ii) the mineralization is slightly
341 slower in the simulated matrix owing to the partial consumption of H₂O₂, Fe²⁺ and
342 •OH/M(•OH) by active chlorine, as well as to the formation of refractory chloroderivatives.⁴⁴



344 The electrochemical characterization by LSV revealed the absence of direct anodic
345 oxidation of bronopol, since no peak appeared before O₂ evolution when using BDD, Pt or
346 DSA as the working electrode. Therefore, hydroxyl radicals are the main oxidant species in
347 trials of Figure 3. The same effects were observed for bronopol decay, as shown in Figure 3a,
348 where EF treatment in Na₂SO₄ yielded the quickest destruction, although quite similar to that
349 found in the other cases. Bronopol disappeared after ca. 300 min following a pseudo-first-
350 order kinetics, with apparent rate constant increasing from 0.014 min⁻¹ for EO-H₂O₂ in
351 simulated water to 0.019 min⁻¹ for EF in 10 mM Na₂SO₄. GC-MS analysis confirmed the
352 disappearance of the parent pollutant at that time, as well as the formation of
353 bromonitromethane as the main oxidation product. This and other minor compounds are
354 responsible for the residual TOC after 300 min (Figure 3a).

355 The fate of Br contained in bronopol during the previous trials was investigated by IC.
356 As an example, Figure 3c shows the time course of all inorganic anions during the EF
357 treatment in 10 mM Na₂SO₄. From the early stages, released Br was accumulated as Br⁻ and
358 BrO₃⁻. Br⁻ concentration reached a maximum value of 0.6 mM at 60 min, whereupon it
359 decreased until disappearing. Simultaneously, BrO₃⁻ concentration increased up to 2.78 mM
360 at the end of the treatment. This suggests that Br is first released as Br⁻, which is further
361 oxidized to bromate by •OH/M(•OH). This kind of conversion is similar to that of Cl⁻ to
362 ClO₄⁻ and that reported under the action of sulfate radicals.^{45,46} The formation of bromate can
363 be basically explained by the attack of hydroxyl radicals, being Cl₂/ClO⁻ irrelevant as
364 deduced from Br⁻ stability shown in the inset of Figure 2.⁴⁷ Note that, at 300 min, the sum of
365 all brominated ions accounted for < 2.78 mM, which confirms the presence of
366 organobrominated by-products until overall mineralization of bronopol solution at 480 min.
367 On the other hand, the entire initial N is transformed into NO₃⁻. Figure S3 in SI depicts the

368 analysis of inorganic anions for EO-H₂O₂. In none of these cases perbromate ions were
369 formed.⁴⁸

370 To gain further understanding on the behavior of Br⁻ ion upon application of EAOPs,
371 the four kinds of anodes were used to treat 2.78 mM NaBr by EO-H₂O₂ and EF. From [Figure](#)
372 [S4a-d in SI](#), it can be concluded that the quick, total conversion of Br⁻ to BrO₃⁻ only occurs
373 with BDD anode, with analogous trends in both EAOPs, thus suggesting that BDD([•]OH) is
374 the main responsible for such transformation. Conversely, the other anodes yielded a much
375 slower conversion, confirming the pivotal role of M([•]OH) to oxidize bromate. Solutions of
376 2.78 mM KBrO₃ were electrolyzed under the same conditions and informed about the total
377 stability of BrO₃⁻, which precludes the potential formation of Br⁻ from cathodic reduction, as
378 also commented for EC.

379 **Enhancement of mineralization of bronopol solutions by a sequential**
380 **electrocoagulation/electro-Fenton treatment.** Based on the evidences discussed so far,
381 which confer a significant dual behavior to EC as a separation and transformation technology
382 and corroborate the high oxidation power of EF to mineralize bronopol by-products, a
383 sequential treatment was proposed.

384 A 2.78 mM bronopol solution, electrocoagulated in simulated water at natural pH under
385 optimum conditions as in [Figure 1b](#), was filtered to collect the supernatant. Afterwards, the
386 solution pH was adjusted to 3.0 with HClO₄ to avoid introducing reactive ions. As can be seen
387 in [Figure 4a](#), TOC was 75 mg/L, whereas ICP measurements confirmed that dissolved iron
388 concentration was 11 mg/L. The EF post-treatment was then carried out in an undivided cell
389 equipped with an air-diffusion cathode and different anode materials at 100 mA. Pt, IrO₂-
390 based and RuO₂-based anodes did not yield a significant TOC removal, which means that the
391 electrocoagulated solution contained very refractory organic compounds. Furthermore, as
392 shown in [SI Figure S2](#), these three anodes yielded the lowest H₂O₂ concentration. Therefore,

393 not only the $M(\bullet\text{OH})$ formed at these anodes are relatively weak oxidants, but the amounts of
394 $\bullet\text{OH}$ formed in the bulk from Fenton's reaction are rather low. In contrast, EC/EF-BDD
395 yielded an 85% TOC removal at 420 min of global treatment. This value is similar to that
396 reported in This value is quite similar to that reported in Figure 3a for EF-BDD at the same
397 time, which is very interesting from an application standpoint, when high organic loads and
398 large volumes have to be treated. Under such conditions, EF finds it difficult to control the
399 stability and progress of the treatment unless the solution to be treated is first diluted, since
400 temperature rises steeply and gas evolves considerably.⁴⁹ Hence, EC would act as a
401 convenient conditioning pre-treatment.

402 [Figure 4b](#) depicts the time course of the main reaction by-product accumulated during
403 the sequential treatment with BDD. After 60 min of optimal EC, formic acid attains 43 mg/L,
404 but this value increased during EF because other organic by-products were progressively
405 oxidized to this acid. Its maximum concentration in EF is 79 mg/L, whereupon it gradually
406 disappeared under the action of $\bullet\text{OH}$ and BDD($\bullet\text{OH}$). Note that other organic by-products are
407 also accumulated in solution, since the maximum amount of formic acid only accounted for
408 21 mg/L TOC. Glycolic acid was reported in the literature,³⁶ but it was not formed during the
409 present trials. Oxalic, tartronic, ketomalonic, acetic and malonic were not formed either.

410 Based on all the information, the reaction pathway for the degradation of bronopol in
411 simulated water by the best sequential electrochemical treatment is proposed in [Figure 5](#). The
412 pollutant is transformed into bromonitromethane in EC, with release of formaldehyde. The
413 former by-product can be converted into bromochloromethane by active chlorine, whereas
414 formaldehyde is oxidized to formic acid, which remains in solution along with Br^- and NO_3^-
415 at 60 min. Coupling EC and EF-BDD allows the gradual mineralization of both, formic acid
416 to CO_2 and H_2O , and Br^- to BrO_3^- , under the action of hydroxyl radicals.

417 It is then evident from this article that, despite more than a century of technological
418 development, some of the fundamentals of EC still remain unknown, which is mainly due to
419 the purely heuristic approach.⁵⁰ Although the viability of EC has been proven even at
420 industrial scale, gaining understanding on the mechanisms and reactivity will open the door to
421 a more rigorous scale-up, with new devices like the sequential EC/EAOPs that is foreseen as a
422 powerful solution to water treatment.

423 **ASSOCIATED CONTENT**

424 Supporting Information (SI) contains Text S1-S5, and Figures S1-S4. This information
425 is available free of charge via the Internet at <http://pubs.acs.org>.

426 **ACKNOWLEDGMENT**

427 Financial support from project CTQ2013-48897-C2-1-R (MINECO, FEDER, EU), as
428 well as from excellence network E3TECH under project CTQ2015-71650-RDT (MINECO) is
429 acknowledged. The authors also thank financial support from MINECO under the FPI grant
430 and the mobility grant EEBB-I-15-10094 to E. Bocos.

431

432 **REFERENCES**

433 (1) Vik, E. A.; Carlson, D. A.; Eikum, A. S.; Gjessing, E. T. Electrocoagulation of potable
434 water. *Water Res.* **1984**, *18* (11), 1355-1360; DOI 10.1016/0043-1354(84)90003-4.

435 (2) Cañizares, P.; Martínez, F.; Jiménez, C.; Lobato, J.; Rodrigo, M. A. Coagulation and
436 electrocoagulation of wastes polluted with dyes. *Environ. Sci. Technol.* **2006**, *40* (20), 6418-
437 6424; DOI 10.1021/es0608390.

438 (3) Lin, H.; Wang, Y.; Niu, J.; Yue, Z.; Huang, Q. Efficient sorption and removal of
439 perfluoroalkyl acids (PFAAs) from aqueous solution by metal hydroxides generated in situ by
440 electrocoagulation. *Environ. Sci. Technol.* **2015**, *49* (17), 10562-10569; DOI
441 10.1021/acs.est.5b02092.

442 (4) Valero, D.; Ortiz, J. M.; Expósito, E.; Montiel, V.; Aldaz, A. Electrocoagulation of a
443 synthetic textile effluent powered by photovoltaic energy without batteries: direct connection
444 behaviour. *Sol. Energy Mater. Sol. Cells* **2008**, *92* (3), 291-297; DOI
445 10.1016/j.solmat.2007.09.006.

446 (5) Holt, P. K.; Barton, G. W.; Mitchell, C. A. The future for electrocoagulation as a
447 localised water treatment technology. *Chemosphere* **2005**, *59* (3), 355-367; DOI
448 10.1016/j.chemosphere.2004.10.023.

449 (6) Brillas, E.; Martínez-Huitle, C. A. Decontamination of wastewaters containing
450 synthetic organic dyes by electrochemical methods. An updated review. *Appl. Catal. B:
451 Environ.* **2015**, *166-167*, 603-643; DOI 10.1016/j.apcatb.2014.11.016.

452 (7) Thiam, A.; Zhou, M.; Brillas, E.; Sirés, I. Two-step mineralization of Tartrazine
453 solutions: Study of parameters and by-products during the coupling of electrocoagulation with
454 electrochemical advanced oxidation processes. *Appl. Catal. B: Environ.* **2014**, *150-151*, 116-
455 125; DOI 10.1016/j.apcatb.2013.12.011.

- 456 (8) Hernández-Ortega, M.; Ponziak, C.; Barrera-Díaz, C.; Rodrigo, M. A.; Roa-Morales,
457 G.; Bilyeu, B. Use of a combined electrocoagulation-ozone process as a pre-treatment for
458 industrial wastewater. *Desalination* **2010**, *250* (1), 144-149; DOI
459 10.1016/j.desal.2008.11.021.
- 460 (9) Boroski, M.; Rodrigues, A. C.; Garcia, J. C.; Gerola, A. P.; Nozaki, J.; Hioka, N. The
461 effect of operational parameters on electrocoagulation-flotation process followed by
462 photocatalysis applied to the decontamination of water effluents from cellulose and paper
463 factories. *J. Hazard. Mater.* **2009**, *160* (1), 448-454; DOI 10.1016/j.jhazmat.2008.02.094.
- 464 (10) Roa-Morales, G.; Campos-Medina, E.; Aguilera-Cotero, J.; Bilyeu, B.; Barrera-
465 Díaz, C. Aluminium electrocoagulation with peroxide applied to wastewater from pasta and
466 cookie processing. *Sep. Purif. Technol.* **2007**, *54* (1), 124-129; DOI
467 10.1016/j.seppur.2006.08.025.
- 468 (11) Chaplin, B. P. Critical review of electrochemical advanced oxidation processes for
469 water treatment applications. *Environ. Sci. Processes Impacts* **2014**, *16* (6), 1182-1203; DOI
470 10.1039/c3em00679d.
- 471 (12) Sirés, I.; Brillas, E.; Oturan, M. A.; Rodrigo, M. A.; Panizza, M. Electrochemical
472 advanced oxidation processes: Today and tomorrow. A review. *Environ. Sci. Pollut. Res.*
473 **2014**, *21* (14), 8336-8367; DOI 10.1007/s11356-014-2783-1.
- 474 (13) Martínez-Huitle, C. A.; Rodrigo, M. A.; Sirés, I.; Scialdone, O. Single and coupled
475 electrochemical processes and reactors for the abatement of organic water pollutants: A
476 critical review. *Chem. Rev.* **2015**, *115* (24), 13362-13407; DOI
477 10.1021/acs.chemrev.5b00361.
- 478 (14) Brillas, E.; Sirés, I.; Oturan, M. A. Electro-Fenton process and related
479 electrochemical technologies based on Fenton's reaction chemistry. *Chem. Rev.* **2009**, *109*
480 (12), 6570-6631; DOI 10.1021/cr900136g.

- 481 (15) Panizza, M.; Cerisola, G. Direct and mediated anodic oxidation of organic
482 pollutants. *Chem. Rev.* **2009**, *109* (12), 6541-6569; DOI 10.1021/cr9001319.
- 483 (16) Dirany, A.; Sirés, I.; Oturan, N.; Özcan, A.; Oturan, M. A. Electrochemical
484 treatment of the antibiotic sulfachloropyridazine: Kinetics, reaction pathways, and toxicity
485 evolution. *Environ. Sci. Technol.* **2012**, *46* (7), 4074-4082; DOI 10.1021/es204621q.
- 486 (17) Olvera-Vargas, H.; Oturan, N.; Brillas, E.; Buisson, D.; Esposito, G.; Oturan, M. A.
487 Electrochemical advanced oxidation for cold incineration of the pharmaceutical ranitidine:
488 Mineralization pathway and toxicity evolution. *Chemosphere* **2014**, *117* (1), 644-651; DOI
489 10.1016/j.chemosphere.2014.09.084.
- 490 (18) Scialdone, O.; Galia, A.; Sabatino, S. Abatement of Acid Orange 7 in macro and
491 micro reactors. Effect of the electrocatalytic route. *Appl. Catal. B: Environ.* **2014**, *148-149*,
492 473-483; DOI 10.1016/j.apcatb.2013.11.005.
- 493 (19) Bocos, E.; Alfaya, E.; Iglesias, O.; Pazos, M.; Sanromán, M. A. Application of a
494 new sandwich of granular activated and fiber carbon as cathode in the electrochemical
495 advanced oxidation treatment of pharmaceutical effluents. *Sep. Purif. Technol.* **2015**, *151*,
496 243-250; DOI 10.1016/j.seppur.2015.07.048.
- 497 (20) El-Ghenymy, A.; Centellas, F.; Rodríguez, R. M.; Cabot, P. L.; Garrido, J. A.; Sirés,
498 I.; Brillas, E. Comparative use of anodic oxidation, electro-Fenton and photoelectro-Fenton
499 with Pt or boron-doped diamond anode to decolorize and mineralize Malachite Green oxalate
500 dye. *Electrochim. Acta* **2015**, *182*, 247-256; DOI 10.1016/j.electacta.2015.09.078.
- 501 (21) Bocos, E.; Pazos, M.; Sanromán, M. A. Electro-Fenton treatment of imidazolium-
502 based ionic liquids: kinetics and degradation pathways. *RSC Adv.* **2016**, *6* (3), 1958-1965;
503 DOI 10.1039/c5ra24070k.
- 504 (22) Thiam, A.; Brillas, E.; Garrido, J. A.; Rodríguez, R. M.; Sirés, I. Routes for the
505 electrochemical degradation of the artificial food azo-colour Ponceau 4R by advanced

506 oxidation processes. *Appl. Catal. B: Environ.* **2016**, *180*, 227-236; DOI
507 10.1016/j.apcatb.2015.06.039.

508 (23) Bocos, E.; Pazos, M.; Sanromán, M. A. Electro-Fenton decolourization of dyes in
509 batch mode by the use of catalytic activity of iron loaded hydrogels. *J. Chem. Technol.*
510 *Biotechnol.* **2014**, *89*, 1235-1242; DOI 10.1002/jctb.4374.

511 (24) Subba Rao, A. N.; Venkatarangaiah, V. T. Metal oxide-coated anodes in wastewater
512 treatment. *Environ. Sci. Pollut. Res.* **2014**, *21* (5), 3197-3217; DOI 10.1007/s11356-013-
513 2313-6.

514 (25) Wu, W.; Huang, Z. -H.; Lim, T. -T. Recent development of mixed metal oxide
515 anodes for electrochemical oxidation of organic pollutants in water. *Appl. Catal. A: General*
516 **2014**, *480*, 58-78; DOI 10.1016/j.apcata.2014.04.035.

517 (26) Tovar-Facio, J.; Lira-Barragán, L. F.; Nápoles-Rivera, F.; Bamufleh, S. S.; Ponce-
518 Ortega, J. M.; El-Halwagi, M. M. Optimal synthesis of refinery property-based water
519 networks with electrocoagulation treatment systems. *ACS Sustain. Chem. Eng.* **2016**, *4* (1),
520 147-158; DOI 10.1021/acssuschemeng.5b00902.

521 (27) Raju, G. B.; Karuppiyah, M. T.; Latha, S. S.; Parvathy, S.; Prabhakar, S. Treatment of
522 wastewater from synthetic textile industry by electrocoagulation-electrooxidation. *Chem. Eng.*
523 *J.* **2008**, *144* (1), 51-58; DOI 10.1016/j.cej.2008.01.008.

524 (28) Panizza, M.; Cerisola, G. Applicability of electrochemical methods to carwash
525 wastewaters for reuse. Part 2: Electrocoagulation and anodic oxidation integrated process. *J.*
526 *Electroanal. Chem.* **2010**, *638* (2), 236-240; DOI 10.1016/j.jelechem.2009.11.003.

527 (29) Cotillas, S.; Llanos, J.; Cañizares, P.; Mateo, S.; Rodrigo, M. A. Optimization of an
528 integrated electrodisinfection/electrocoagulation process with Al bipolar electrodes for urban
529 wastewater reclamation. *Water Res.* **2013**, *47* (5), 1741-1750; DOI
530 10.1016/j.watres.2012.12.029.

- 531 (30) Thiam, A.; Zhou, M.; Brillas, E.; Sirés, I. A first pre-pilot plant for the combined
532 treatment of dye pollutants by electrocoagulation/EAOPs. *J. Chem. Technol. Biotechnol.*
533 **2014**, 89 (8), 1136-1144; DOI 10.1002/jctb.4358.
- 534 (31) Picón-Camacho, S. M.; Taylor, N. G.; Bron, J. E.; Guo, F. C.; Shinn, A. P. Effects of
535 long duration, low dose bronopol exposure on the control of *Ichthyophthirius multifiliis*
536 (*Ciliophora*), parasitising rainbow trout (*Oncorhynchus mykiss* Walbaum). *Vet. Parasitol.*
537 **2012**, 186 (3-4), 237-244; DOI 10.1016/j.vetpar.2011.11.022.
- 538 (32) Kireche, M.; Peiffer, J. -L.; Antonios, D.; Fabre, I.; Giménez-Arnau, E.; Pallardy,
539 M.; Lepoittevin, J. -P.; Ourlin, J. -C. Evidence for chemical and cellular reactivities of the
540 formaldehyde releaser bronopol, independent of formaldehyde release. *Chem. Res. Toxicol.*
541 **2011**, 24 (12), 2115-2128; DOI 10.1021/tx2002542.
- 542 (33) European Commission, Council Directive 76/768/EEC of 27 July 1976 on the
543 approximation of the laws of the member states relating to cosmetic products, **2007**.
- 544 (34) Carbajo, J. B.; Perdigón-Melón, J. A.; Petre, A. L.; Rosal, R.; Letón, P.; García-
545 Calvo, E. Personal care product preservatives: Risk assessment and mixture toxicities with an
546 industrial wastewater. *Water. Res.* **2015**, 72, 174-185; DOI 10.1016/j.watres.2014.12.040.
- 547 (35) Cui, N.; Zhang, X.; Xie, Q.; Wang, S.; Chen, J.; Huang, L.; Qiao, X.; Li, X.; Cai, X.
548 Toxicity profile of labile preservative bronopol in water: The role of more persistent and toxic
549 transformation products. *Environ. Pollut.* **2011**, 159 (2), 609-615; DOI
550 10.1016/j.envpol.2010.09.036.
- 551 (36) Matczuk, M.; Obarski, N.; Mojski, M. The impact of the various chemical and
552 physical factors on the degradation rate of bronopol. *Int. J. Cosmet. Sci.* **2012**, 34 (5), 451-
553 457; DOI 10.1111/j.1468-2494.2012.00730.x.
- 554 (37) Welcher, F. J., Ed. *Standard Methods of Chemical Analysis*, 6th. ed., vol. 2, part B, p.
555 1827; R.E. Krieger Publishing Co.: Huntington, New York, 1975.

- 556 (38) APWA, AWWA and WEF. Method number 4500-Cl Chlorine (residual) – G. DPD
557 Colorimetric Method. In *Standard Methods for the Examination of Water and Wastewater*;
558 21st Ed.; American Public Health Association: Washington D.C. **2005**; pp. 4-67 to 4-68.
- 559 (39) Candeias, L. P.; Stanford, M. R. L.; Wardman, P. Formation of hydroxyl radicals on
560 reaction of hypochlorous acid with ferrocyanide, a model iron(II) complex. *Free Radic. Res.*
561 **1994**, *20* (4), 241-249; DOI 10.3109/10715769409147520.
- 562 (40) Kishimoto, N.; Nakamura, Y.; Kato, M.; Otsu, H. Effect of oxidation-reduction
563 potential on an electrochemical Fenton-type process. *Chem. Eng. J.* **2015**, *260*, 590-595; DOI
564 10.1016/j.cej.2014.09.056.
- 565 (41) Wang, H.; Provan, G. J.; Helliwell, K. Determination of bronopol and its
566 degradation products by HPLC. *J. Pharm. Biomed. Anal.* **2002**, *29* (1-2), 387-392; DOI
567 10.1016/S0731-7085(02)00078-X.
- 568 (42) Thiam, A.; Brillas, E.; Centellas, F.; Cabot, P. L.; Sirés, I. Electrochemical reactivity
569 of Ponceau 4R (food additive E124) in different electrolytes and batch cells. *Electrochim.*
570 *Acta* **2015**, *173*, 523-533; DOI 10.1016/j.electacta.2015.05.085.
- 571 (43) Kraft, A. Doped diamond: A compact review on a new, versatile electrode material.
572 *Int. J. Electrochem. Sci.* **2007**, *2* (5), 355-385.
- 573 (44) Thiam, A.; Sirés, I.; Brillas, E. Treatment of a mixture of food color additives (E122,
574 E124 and E129) in different water matrices by UVA and solar photoelectro-Fenton. *Water*
575 *Res.* **2015**, *81*, 178-187; DOI 10.1016/j.watres.2015.05.057.
- 576 (45) Sánchez-Carretero, A.; Sáez, C.; Cañizares, P.; Rodrigo, M. A. Electrochemical
577 production of perchlorates using conductive diamond electrolyses. *Chem. Eng. J.* **2011**, *166*
578 (2), 710-714; DOI 10.1016/j.cej.2010.11.037.

579 (46) Fang, J. -Y.; Shang, C. Bromate formation from bromide oxidation by the
580 UV/persulfate process. *Environ. Sci. Technol.* **2012**, *46* (16), 8976-8983; DOI
581 10.1021/es300658u.

582 (47) Bouland, S.; Duguet, J. P.; Montiel, A. Evaluation of bromate ions level introduced
583 by sodium hypochlorite during post-disinfection of drinking water. *Environ. Technol.* **2005**,
584 *26* (2), 121-126; DOI 10.1080/09593332608618572.

585 (48) Sáez, C.; Cañizares, P.; Sánchez-Carretero, A.; Rodrigo, M. A. Electrochemical
586 synthesis of perbromate using conductive diamond anodes. *J. Appl. Electrochem.* **2010**, *40*
587 (10), 1715-1719; DOI 10.1007/s10800-010-0108-8.

588 (49) Boye, B.; Farnia, G.; Sandonà, G.; Buso, A.; Giomo, M. Removal of vegetal tannins
589 from wastewater by electroprecipitation combined with electrogenerated Fenton oxidation. *J.*
590 *Appl. Electrochem.* **2005**, *35* (4), 369-374; DOI 10.1007/s10800-005-0797-6.

591 (50) Moreno-Casillas, H. A.; Cocke, D. L.; Gomes, J. A. G.; Morkovsky, P.; Parga, J. R.;
592 Peterson, E. Electrocoagulation mechanism for COD removal. *Sep. Purif. Technol.* **2007**, *56*
593 (2), 204-211; DOI 10.1016/j.seppur.2007.01.031.

594

595 **Figure captions**

596 **Figure 1.** (a) Effect of experimental variables (electrode pairs and interelectrode gap) on
597 percentage of TOC removal vs. applied current for the EC treatment of 150 mL of 2.78 mM
598 bronopol in simulated water at natural pH using Fe as the anode and cathode. (b) TOC
599 abatement with electrolysis time for the optimum EC treatment with 2 Fe/Fe pairs separated
600 1.0 cm at 200 mA.

601 **Figure 2.** Time course of bronopol content for the optimum EC process shown in Figure 1b.
602 The inset panel presents the evolution of Br^- concentration during the trial.

603 **Figure 3.** (a) TOC decay vs. electrolysis time for the EO- H_2O_2 and EF (with 0.50 mM Fe^{2+})
604 treatments of 100 mL of 2.78 mM bronopol in simulated water and in 10 mM Na_2SO_4 at pH
605 3.0 using a BDD/air-diffusion cell at 100 mA. (b) Bronopol concentration abatement and
606 pseudo-first order kinetic analysis in the inset panel for the above assays. (c) Evolution of
607 inorganic ions released during the above EF treatment with 10 mM Na_2SO_4 .

608 **Figure 4.** (a) Variation of TOC with electrolysis time for solutions of 2.78 mM bronopol
609 degraded by sequential treatment: EC (150 mL simulated water, natural pH, 2 Fe/Fe pairs
610 separated 1.0 cm, 200 mA) followed by EF (100 mL, pH 3.0, 100 mA) with several anodes
611 and an air-diffusion cathode. (b) Time course of formic acid detected during this sequential
612 EC/EF-BDD process.

613 **Figure 5.** Reaction pathway for total bronopol mineralization by the best sequential treatment
614 (EC/EF-BDD).

615

616
617
618
619
620
621
622
623
624
625
626
627
628
629
630
631
632
633
634
635
636
637
638

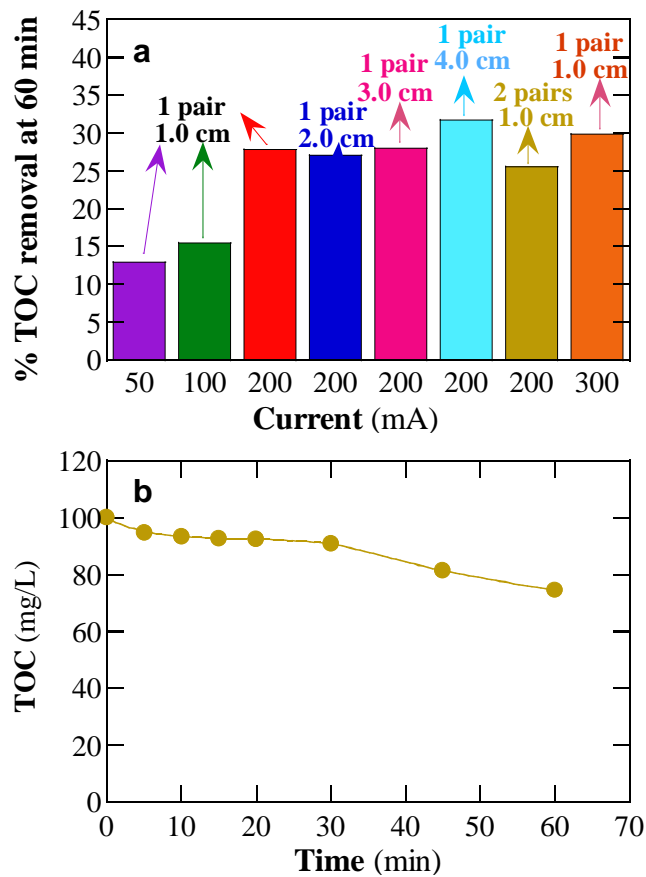


Figure 1

639
640
641
642
643
644
645
646
647
648
649
650
651
652
653
654

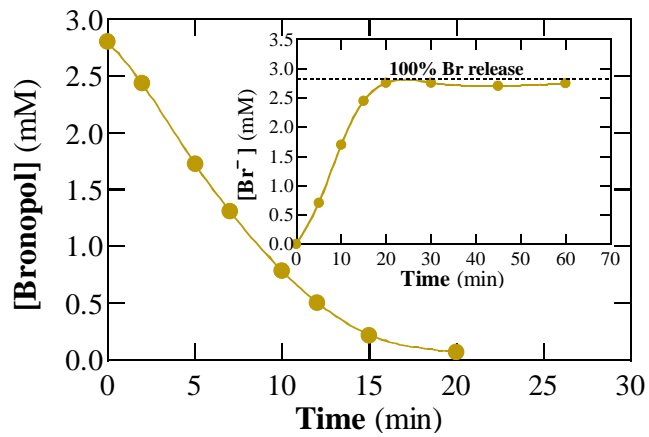


Figure 2

655
656
657
658
659
660
661
662
663
664
665
666
667
668
669
670
671
672
673
674
675
676
677
678
679

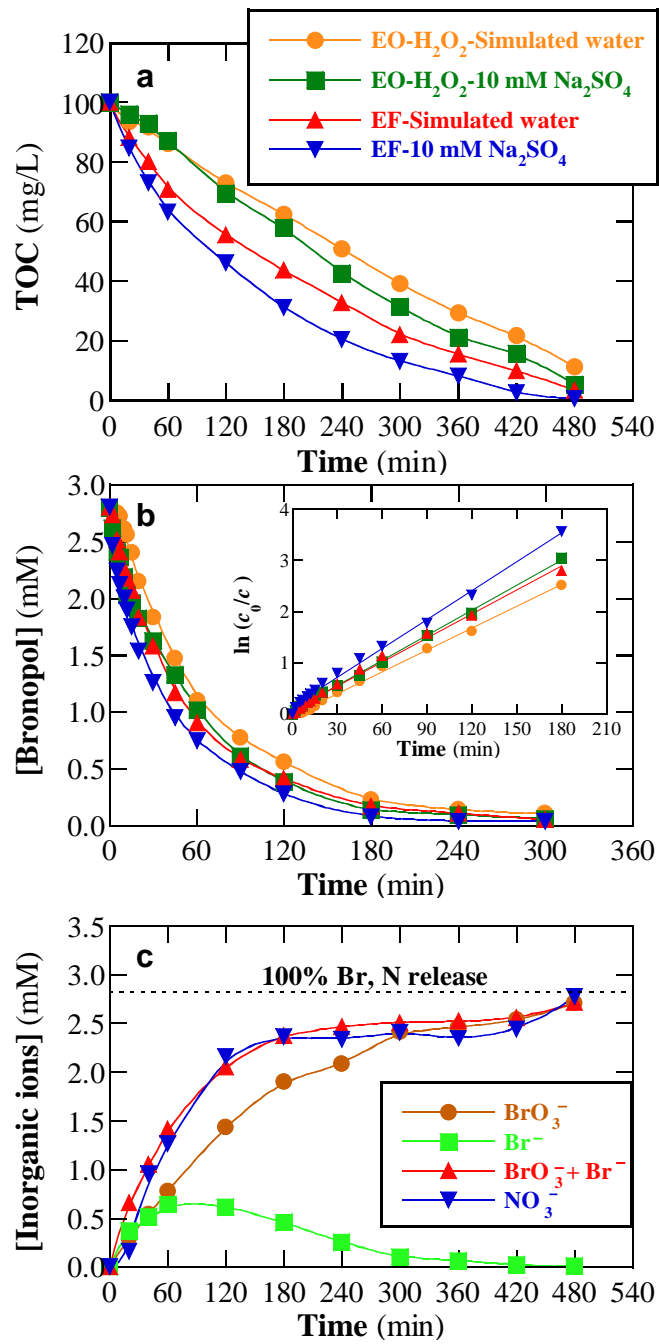


Figure 3

680
681
682
683
684
685
686
687
688
689
690
691
692
693
694
695
696
697
698
699

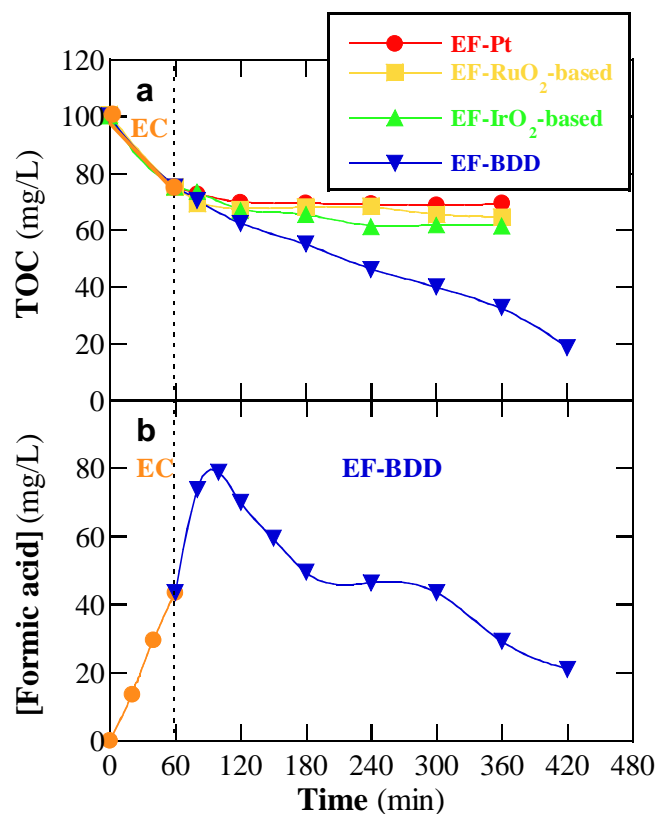
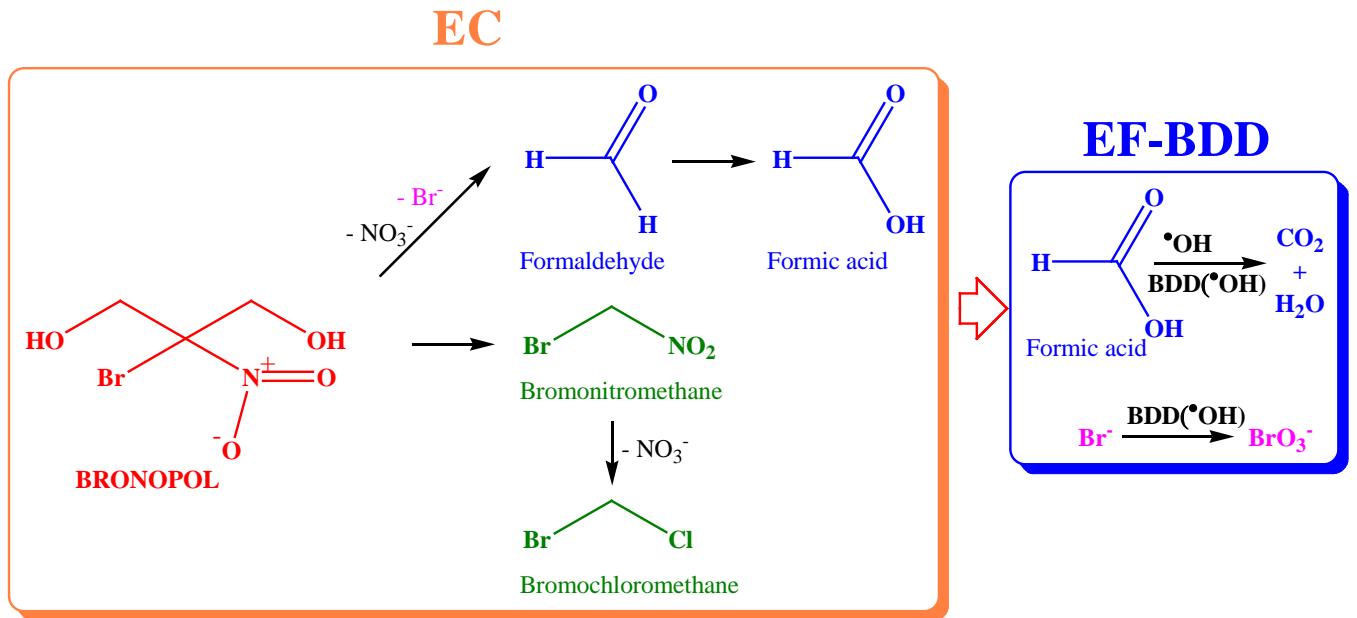


Figure 4

700
701
702
703



704
705
706
707
708
709
710

Figure 5